Colloid Polym Sci 278:629–636 (2000)

ORIGINAL CONTRIBUTION

B. Hoffmann
J. Kressler
G. Stöppelmann
Chr. Friedrich
G.-M. Kim

Rheology of nanocomposites based on layered silicates and polyamide-12

Received: 23 April 1999
Accepted: 22 December 1999

B. Hoffmann · Chr. Friedrich
Institut für Makromolekulare Chemie und
Freiburger Materialforschungszentrum
Albert-Ludwigs-Universität
Stefan-Meier-Strasse 21
79104 Freiburg, Germany

J. Kressler (✉)
Martin-Luther-Universität
Halle-Wittenberg
Fachbereich Ingenieurwissenschaften
06099 Halle (Saale), Germany
e-mail: joerg.kressler@iw.uni-halle.de
Tel.: +49-3461-462760
Fax: +49-3461-462592

G. Stöppelmann
EMS-Chemie AG, 7013 Domat/Ems
Switzerland

G.-M. Kim
Eindhoven University of Technology
Faculty of Mechanical Engineering-Section
Materials Technology
5600 MB Eindhoven
The Netherlands

Abstract Nanocomposites based on polyamide-12 (PA-12) and layered silicates are synthesized and analyzed with respect to their morphological and rheological properties. Transmission electron microscopy shows the fine dispersion of silicate layers in a PA-12 matrix. Different swelling agents for the clay (protonated aminododecanoic acid or water) are used. This allows the molar mass of PA-12 to be controlled during the preparation of the nanocomposites. When aminododecanoic acid is used as a swelling agent, the exfoliated silicate layers are chemically bonded to the matrix, whereas the use of water as a swelling agent leads to exfoliated silicate layers well dispersed in the polymer matrix without tethered polymer chains. The rheological behavior of the nanocomposites differs extremely from that of the pure PA-12 matrices. A qualitative description of the rheology of these nanocomposites is provided.

Key words Nanocomposites · Polyamide · Clay · Rheology

Introduction

The addition of fillers to polymers expands their range of application [1]. In many cases fillers such as glass beads, $CaCO_3$ or $BaSO_4$, which have a very low aspect ratio, are employed. The mechanical properties may be widely improved by fillers having a large aspect ratio. Such materials are, for example, short fibers, mica or talc. The dimensions of these fillers are usually in the micrometer range. The improvement of mechanical properties might be more effective with fillers in the nanometer range. (2:1)-three layered silicate, such as montmorillonite or hectorite, are known as good nanofillers because they can be separated into single sheets with a thickness of approximately 1 nm. Large amounts of water can be loaded in the interlayer spacing or the Na^+ and Li^+ cations can be replaced with organic cations, for example, $R\text{-}NH_3^+$ [2–4]. A prerequisite to obtain a nanocomposite with highly improved properties is a fine dispersion on the exfoliated silicate layers [5–8]. This is usually achieved by appropriate swelling techniques, followed by a compounding step or in situ polymerization. In the last decades the preparation of a great variety of nanocomposites has been reported in the literature [9–23]. These nanocomposites were usually characterized by means of wide angle X-ray scattering (WAXS), transmission electron microscopy (TEM) and mechanical testing. It was described how the interlayer distance increases during the swelling of the silicates characterized by a shift in the d_{001} reflection in the WAXS traces towards smaller 2Θ values. Sometimes this reflection disappears completely. This is also the case when the layered silicate is completely dispersed in a polymer matrix. The TEM measurements occasionally depict larger agglomerates of layered silicates with an increased interlayer distance [21]. Usually, nanocomposites show increased Young's moduli but simultaneously also a loss in impact toughness. The ultimate goal to achieve materials with both high stiffness and high toughness can only be realized in exceptional cases [8–11]. In previous work we demonstrated for polyamide-12 (PA-12) nanocomposites that it is possible to obtain materials with increased stiffness (Young's modulus) without sacrificing the high notched impact toughness [24].

The rheological properties of in situ polymerized nanocomposites with end-tethered polymer chains were first described by Giannelis and coworkers [25, 26]. The flow behavior of poly(ε-caprolactone) (PCL) and polyamide-6 (PA-6) nanocomposites differed extremely from that of the neat matrices. The slope of the storage modulus, G', and the loss modulus, G'', versus the frequency, ω, in the terminal region was smaller than 2 and 1, respectively. Values of 2 and 1 are expected for melts of linear monodispers polymers [27, 28]. Furthermore, it was shown that the Arrhenius activation energy is not influenced by the addition of layered silicate to PCL in comparison to the neat polymer [26]. However, the thermorheological behavior of PA-6 nanocomposites was not investigated.

The aim of this work is to investigate the rheological properties of PA-12 nanocomposites at different temperatures in order to verify the time–temperature superposition principle. The rheological behavior is studied as a function of the degree of filling, as a function of the method of swelling of the clay and as a function of the molar mass of the polymer matrix. A qualitative model is proposed in order to describe the changes in the rheological behavior in nanocomposites compared to those in neat polymers.

Experimental

Silicates

Two kinds of layered silicates were used: a synthetic and a natural silicate. The synthetic silicate SOMASIF ME100 (layered silicate A: LSA, 26.5 wt% Si; 15.6 wt% Mg; 0.2 wt% Al; 4.1 wt% Na; 0.1 wt% Fe; 3.8 F), which represents a fluoromica and was prepared by heating talcum in the presence of Na_2SiF_6, was obtained from CO-OP, Japan. The negative charge of the layers is compensated by Na^+ ions in the interlayer space. The cation-exchange capacity (CEC) is in a range of 0.7–0.8 mEq/g for LSA [29]. The natural silicate (bentonite, layered silicate B: LSB) was supplied by Süd-Chemie, Germany. LSB is a mixture of differently sized silicates, mainly montmorillonite (more than 80%) with by-products such as quartz, mica, chlorite and feldspar [30–32]. The CEC is in a range of 0.7–1.0 mEq/g for LSB. The interlayer spacing calculated from the WAXS d_{001} reflection is 0.95 nm for LSA and LSB, respectively [29, 30].

ω-Aminododecanoic acid and PA-12

ω-Aminododecanoic acid (ADA) (used for silicate swelling and polycondensation) was provided by EMS-Chemie, Switzerland. Two PA-12 samples were used as reference materials. These PA-12 grades were commercial products from EMS-Chemie (Grilamid) with different molar masses. PAA was a PA-12 sample with a low molar mass and PAB had a high molar mass. The viscosity data and end group analyses are given in Table 1. The melting points are 179 °C, the melting enthalpies are 59 J/g, and the crystallization enthalpies are 56 J/g as determined by differential scanning calorimetry experiments with heating and cooling rates of 10 °C/min. These data are identical for both samples.

Swelling of the layered silicates

LSA was dispersed in water and swollen by three different methods. In method a the overall concentrations were 20 mmol/l ADA, 24 mmol/l HCl and 8.3 g/l LSA. In method b an excess of ADA with respect to the CEC for LSA (overall concentration 40 mmol/l) was added. In method c the HCl concentration was reduced to 4 mmol/l compared to method b. The dispersions were filtered and dried at 80 °C. Additionally, LSB was swollen with water only (method d). A paste of 20 wt% LSB in water was used directly for the polycondensation.

Thermogravimetric analysis

For the thermogravimetric analyses (TGA) 20 mg of the sample was put in a corundum pan. The temperature range was between 30 and 700 °C with a heating rate of 5 °C/min under a nitrogen atmosphere.

Transmission electron microscopy

The morphology of the samples was examined by TEM. For the TEM measurements, ultrathin sections were prepared at −80 °C with an Ultracut E ultramicrotome (Reichert & Jung) using a diamond knife. The measurements were carried out on a Zeiss CEM 912 (120 kV).

WAXS measurements

The swelling of the layered silicates with ADA or water was studied by means of WAXS using a Siemens D500 apparatus with Cu K_α radiation ($\lambda = 0.154$ nm) and a scanning rate of 0.3 °C/min.

Nanocomposites

The nanocomposites were prepared by polycondensation of ADA at 280 °C in an autoclave in the presence of the swollen silicates. After 1 h the pressure was raised to 20 bar. In the subsequent 1.5 h the pressure was continuously reduced to ambient pressure. The mixture was stirred for another 7 h, degassed, pelletized and dried. The nanocomposites are abbreviated NCLSA*i*-*X* or NCLSB*i*-*X*.

Table 1 Interlayer distance of the silicate after the swelling procedure and characteristic data of PA-12 nanocomposites. See text for an explanation of the notation

	Interlayer distance of the silicate (nm)	Silicate loading (wt%)	Relative viscosity[e]	Concentration of COOH end groups (μEq/g)	Concentration of NH_2 end groups (μEq/g)	Calculated M_n[f] (kg/mol)
PAA	–	0	1.6	90	13	11.6
PAB	–	0	2.0	60	25	17.4
NCLSAa-2[a]	1.8	2	2.3	90	5	16.9
NCLSAa-4[a]	1.8	4	1.6	141	7	10.3
NCLSAb-2[b]	2.0	2	2.0	94	5	16.4
NCLSAb-4[b]	2.0	4	1.8	170	11	8.8
NCLSAc-2[c]	2.0	2	2.1	57	30	22.0
NCLSAc-4[c]	2.0	4	1.6	159	6	11.6
NCLSBd-2[d]	Exfoliated	2	1.8	47	52	20.2
NCLSBd-4[d]	Exfoliated	4	1.8	40	59	20.2

[a] Prepared with swollen LSA (20 mmol/l ADA; 24 mmol/l HCl; 8.3 g/l LSA) (method a)

[b] Prepared with swollen LSA (40 mmol/l ADA; 24 mmol/l HCl; 8.3 g/l LSA) (method b)

[c] Prepared with swollen LSA (40 mmol/l ADA; 4 mmol/l HCl; 8.3 g/l LSA) (method c)

[d] Prepared with LSB swollen with water

[e] Relative viscosity determined by the ratio of the viscosity of a 0.5 wt% solution of the polymer in *m*-cresol to the viscosity of pure *m*-cresol at 25 °C

[f] Calculated using Eq. (1); for methods a and b an organic content of 20 wt% is bonded to the layers; [U] = 23 μEq/g (2 wt%); [U] = 46 μEq/g (4 wt%); for method c [U] = 4 μEq/g (2 wt%); [U] = 8 μEq/g (4 wt%); for PAA [U] = 70 μEq/g, for PAB [U] = 30 μEq/g and for LSB [U] = 0 μEq/g

NC means nanocomposite, *i* stands for the swelling method (a, b, c or d) and *X* indicates the inorganic content in weight percent.

Rheological characterization

The pure polyamides and the nanocomposites were dried for 48 h at 60 °C in a vacuum and were melted for 20 min under vacuum at a temperature of 200 °C in a Collin PCS2 vacuum press. The samples were pressed for 10 min and were subsequently quenched to ambient temperature. The plates had a diameter of 25 mm and a thickness of approximately 1 mm. For the rheological measurements a Paar Physica UDS200, a stress-controlled rheometer, with parallel-plate geometry was used. All measurements were carried out under nitrogen. The shear-flow behavior of different molar mass PA-6 samples has been discussed by Pezzin and Gechele [33]. They found an increase in the melt viscosity with holding time. This result was also observed by other groups [34, 35]. A horizontal line in the time sweep plot proved the time stability of our measurements for at least 70 min. For this reason we selected short frequency sweeps ranging from 25 to 1 rad/s. This guaranteed that the materials were stable over the frequency and temperature ranges investigated. The strain/stress region in which the linear viscoelastic properties are valid was determined by amplitude sweep experiments. Each sample was measured at different temperatures ranging from 200 to 240 °C. The temperature was increased in steps of 5 °C. The reference temperature was 210 °C in all cases.

Results and discussion

Usually the preparation of layered silicate is carried out by swelling the silicates during ion exchange using protonated amino acids dispersed in water followed by a polycondensation step. Depending on the swelling method employed, it is also possible to control the interlayer spacing of the layered silicates in the polyamide matrix obtained by polycondensation. Assuming a tube shape for ADA, the diameter is approximately 0.4 nm and the length is approximately 1.9 nm [36]. The interlayer distance after swelling by method a is 1.8 nm compared to the 0.95 nm of the unmodified layered silicate. This correlates with the intercalation of two molecules of ADA placed flat-on between two silicate layers. This is in agreement with literature data [30, 36, 37]. Employing swelling methods b and c leads to an interlayer distance of 2.0 nm. This is an indication that molecules which are not in direct contact with the silicate are intercalated in the interlayer spacing in addition to the two layers of ADA. Swelling methods a–c are connected with the disadvantage of the stoichiometric imbalance caused by the "loss" of amino groups attached via ion bonding to the layered silicate. These effects can be studied readily by end group analysis. In the case where the end groups are expressed in equivalents per million grams of polymer, the number-average molar mass can be calculated using Eq. (1).

$$M_\mathrm{n} = \frac{2 \times 10^6}{[\mathrm{COOH}] + [\mathrm{NH_2}] + [\mathrm{U}]} \tag{1}$$

In Eq. (1) a factor of 2 appears because of the two different end groups. [COOH] is the concentration of acid end groups, [NH_2] is the concentration of amine end groups and [U] is the concentration of regulator. Thus, only acid end groups of protonated and bonded ADA can react in the polycondensation and the acid end groups must be considered as chain-length regulators. The achievable molar mass during polycondensation is therefore decreased. The concentration of the regulator was analyzed by means of TGA. TGA traces of the neat layered silicates do not show any weight loss in the temperature range studied (up to 700 °C). The weight loss of ADA is finished at about 480 °C, also after ion exchange with the layered silicates. These data allow an exact calculation of the loading of the layered silicates with organic material. They are extremely important in order to estimate the amount of chain-length regulator present during the polycondensation as discussed previously. In Table 1 the inorganic content of the nanocomposites from TGA data obtained prior to and after complete decomposition of the polymeric material is listed. In the case where the swelling is carried out using method a or b, the amount of chain-length regulator can be calculated. For a 2 wt% nanocomposite the amount is 23 μEq/g; with 4 wt% layered silicate the value is 46 μEq/g. Using method c the amount of chain-length regulator is approximately 17% smaller, for NCLSAc-2 it is about 4 μEq/g and for NCLSAc-4 it is approximately 8 μEq/g. The molar masses calculated using Eq. (1) are listed in Table 1. The calculated molar masses correlate, at least qualitatively, with the solution viscosity data. The largest molar masses are achieved without chain-length regulators, i.e. when the silicate is swollen in water prior to polycondensation (method d). This method is discussed in more detail later. In the other cases the relative viscosity decreases with increasing amount of chain-length regulator.

Hence, the alternative preparation of nanocomposites in which the LSB is swollen exclusively in water prior to polycondensation is applied. The WAXS trace of LSB after swelling with water is shown in Fig. 1. The d_{001} reflection of LSB which appears at an angle of $2\Theta = 10°$ disappears completely and simultaneously a strong increase in the scattering intensity at angles smaller than $2\Theta = 5°$ occurs. The other reflections for LSB at 2Θ values larger than 18° are still detectable. In conclusion it can be said that the loss of the d_{001} reflection is caused by the exfoliation process resulting in relatively large interlayer spacings with a broad distribution [30]. The exfoliation is caused by the deposition of large amounts of water between the layers.

Prior to rheological investigations, it is absolutely necessary to validate the micromorphology of the nanocomposites. A powerful tool to observe structures in the nanometer range is TEM. Two TEM micrographs of nanocomposites loaded with 2 wt% clay are shown in Fig. 2. The TEM image in Fig. 2A shows a nanocomposite prepared by method b (NCLSAb-2) and in Fig. 2B a nanocomposite prepared by method d (NCLSBd-2) can be seen. The dark entities can be assigned unambiguously to exfoliated silicate layers [24]. Both swelling methods lead to nanocomposites with a well-defined morphology, i.e. several separated silicate sheets can be observed and large silicate particles are absent. This proves especially that clays swollen with water only can be used for the preparation of polyamide nanocomposites in addition to the normal way of swelling the clay mineral in the first step with amino acids.

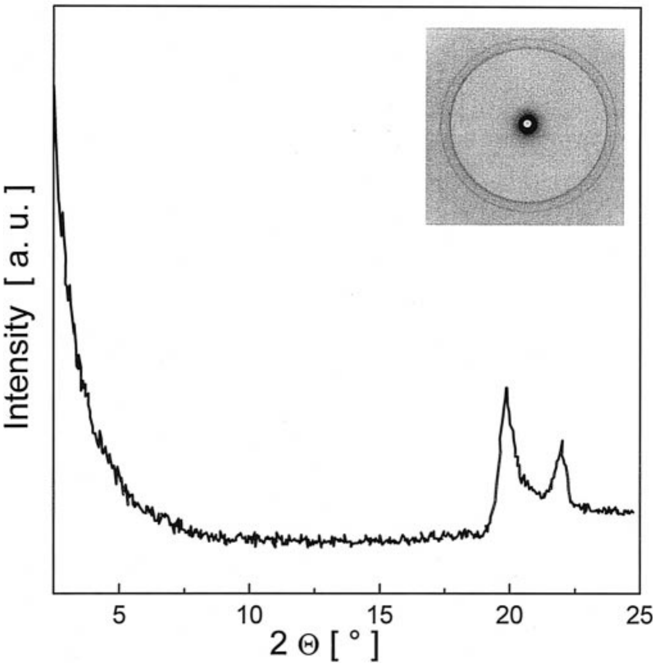

Fig. 1 Wide-angle X-ray scattering trace and 2D image of layered silicate B swollen with water (method d)

After the preparation of nanocomposites over a wide range of molar masses and clay contents and the validation of the silicate layer dispersion in the polymer matrix, it is interesting to study the viscoelastic behavior. There is, of course, an improvement in application properties of nanocomposites compared to the respective neat polymers; however, it can be assumed that the clay loading has a significant influence on the flow behavior of the melt. This needs to be addressed very carefully in order to understand the processability of the new class of materials.

In general, the rheology of polymer melts depends strongly on the temperature. It is well known that in the case of thermorheological simplicity, isotherms of G' and G'' (or other material functions) can be superimposed by horizontal shifts along the frequency axis:

$$G'(\omega\, a_T, T_0) = G'(\omega, T);\; G''(\omega\, a_T, T_0) = G''(\omega, T) \ , \tag{2}$$

where a_T is the horizontal shift factor and T_0 is the reference temperature. All isotherms measured for neat polyamides and for nanocomposites can be superimposed along the frequency axis. a_T for PA-12 and the nanocomposites have comparatively small values in contrast to other thermoplastic polymers such as polystyrene (PS) [27].

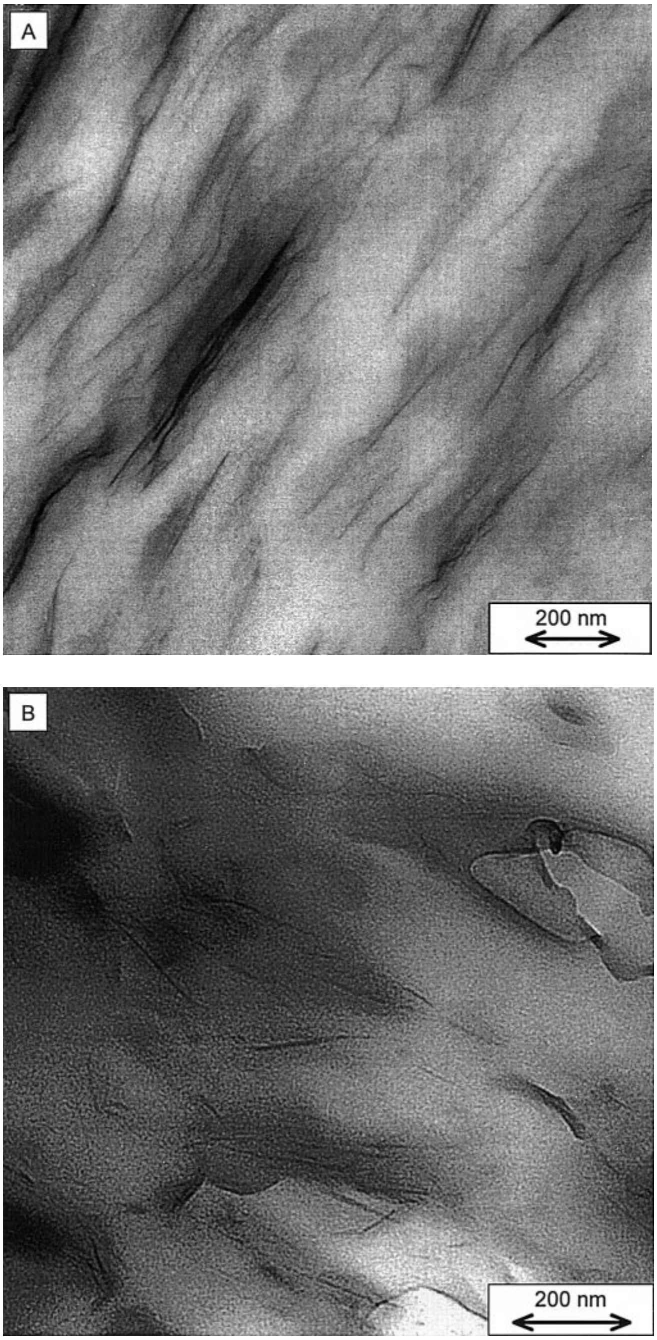

Fig. 2 Transmission electron microscopy micrographs of nanocomposites **A** NCLSAb-2 and **B** NCLSBd-2

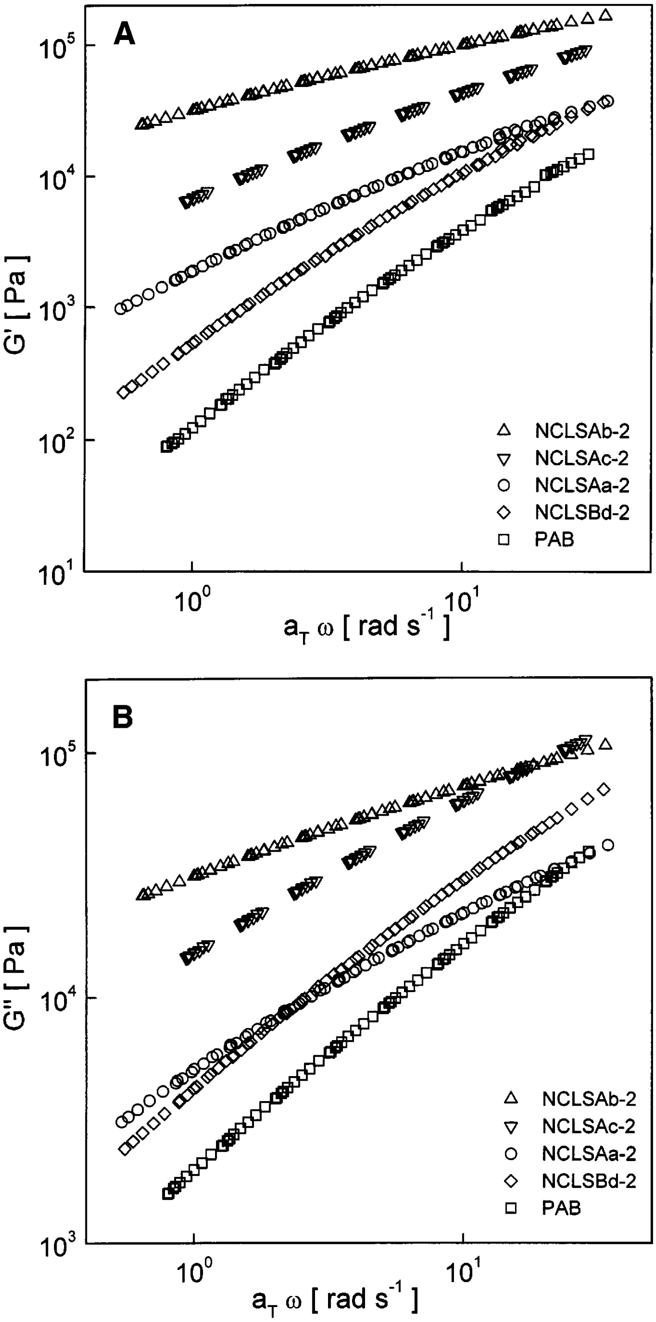

Fig. 3 **A** Storage modulus (*G′*) and **B** loss modulus (*G″*) of PAB, NCLSAa-2, NCLSAb-2, NCLSAc-2 and NCLSBd-2 (T_{Ref} = 210 °C). See text for an explanation of the notation

For polymer samples in the molar mass region under investigation, it is expected that at lower frequencies the polymer chains should be fully relaxed and exhibit characteristic homopolymer-like terminal flow behavior, with slopes of 2 and 1 for *G′* and *G″*, respectively. The master curves for *G′* and *G″* of PAB and of the nanocomposites with 2 wt% silicate loading are shown in Fig. 3. It is clearly recognizable that the master curves of the nanocomposites have a smaller slope in the terminal region for systems in which the layered silicate is ionically bonded to the polymer matrix (upper three curves) compared to a system in which the layered silicate is only dispersed in the matrix (NCLSBd-2) and also compared to pure PAB. The slopes will be discussed later in more detail. Also the moduli in the terminal region are strongly increased for all nanocomposites.

For the systems with 4 wt% silicate loading (Fig. 4), the moduli are generally shifted to smaller modulus values compared to the respective nanocomposites with 2 wt% silicate loading. Since larger amounts of chain length regulators are present during the preparation of the samples with 4 wt% silicate, the molar masses of the matrices are smaller compared to nanocomposites with 2 wt% clay (Table 1). A certain exception is the nanocomposite with a silicate not ionically bonded to the polymer matrix (NCLSBd-4). This nanocomposite shows a clear increase in the moduli when compared to PAA, identical with the increase in the sample with 2 wt% LSB. This is a result of the absence of chain-length regulators. It should be remembered that the silicate swelling for method d was carried out in water only. Hence the moduli for nanocomposites of polyamide with clay which is not chemically bonded to the matrix but is well dispersed in the nanometer range are governed by the molar mass of the polyamide and only to a minor extent by the degree of filling for such small concentrations (e.g. 2 or 4 wt%).

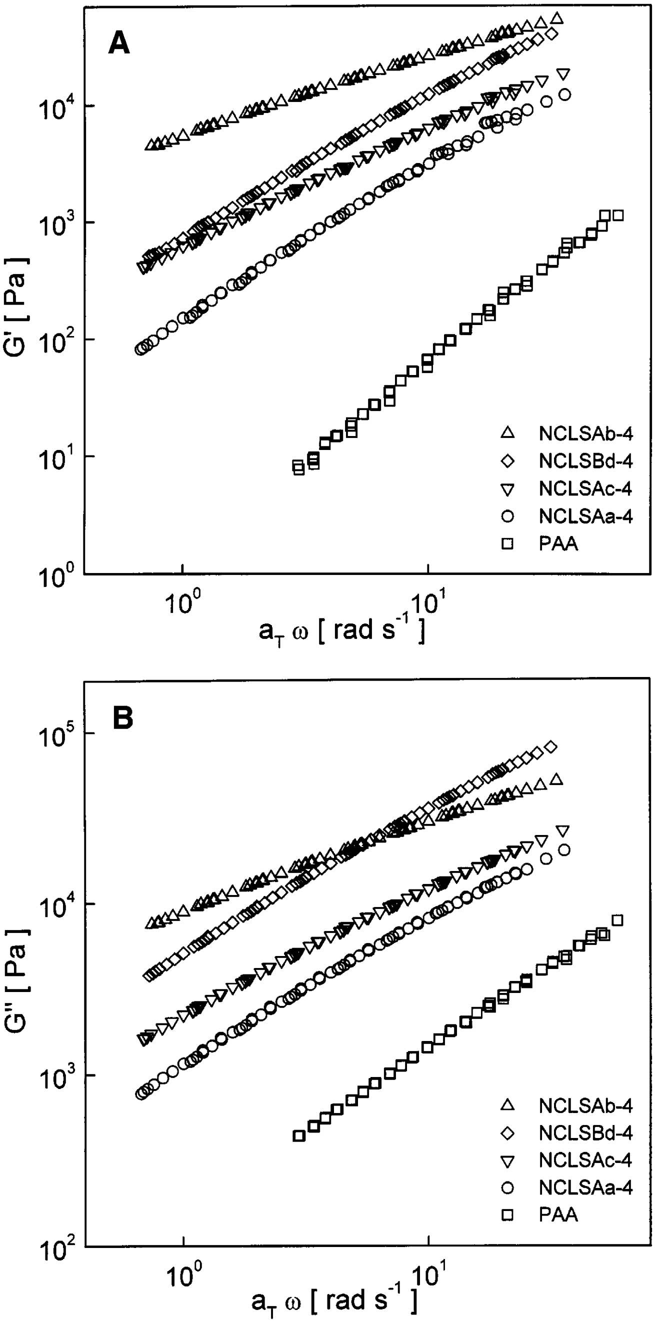

Fig. 4 **A** (*G*′) and **B** (*G*″) of PAA, NCLSAa-4, NCLSAb-4, NCLSAc-4 and NCLSBd-4 (T_{Ref} = 210 °C). See text for an explanation of the notation

The slopes of the terminal regions of the master curves for *G*′ and *G*″ are listed in Table 2. The slopes of *G*′ and *G*″ are lower for all nanocomposites than for pure polyamides. Only the slopes of *G*′ will be discussed here because the effects are more pronounced in *G*′ than in *G*″. The slopes of pure PA-12 (PAB and PAA) are between 1.6 and 1.8. These slopes are in the range expected for polydisperse polymers [38]. NCLSAb-2 and NCLSAb-4 have the smallest slope. For the preparation of these nanocomposites a swollen layered silicate with an interlayer distance of 2.0 nm was used. As can be seen in Table 2, the slopes are in the range between 0.6 and 0.7. For NCLSAc-2 and NCLSAc-4, the slope is approximately 1.1. The largest slope is 1.4 for NCLSAa-4. The slopes and the absolute values of the dynamic moduli indicate a supermolecular structure formation in the nancomposites. The higher the *G*′ moduli and the smaller the slope, the more pronounced the interaction between the silicate platelets and their tendency to form a three-dimensional superstructure. The end-tethered polymer chains on the silicate layers stabilize this superstructure. Rheological measurements performed on PS-based model nanocomposites have shown that the formation of a superstructure goes

Table 2 Slope of *G*′ and *G*″ in the terminal region of the master curves (Figs. 3, 4) of nanocomposites compared to PA-12

	Slope of *G*′	Slope of *G*″
PAA	1.8	1.0
PAB	1.6	1.0
NCLSAa-2	0.9	0.8
NCLSAa-4	1.4	1.0
NCLSAb-2	0.6	0.4
NCLSAb-4	0.7	0.6
NCLSAc-2	1.1	0.8
NCLSAc-4	1.1	0.8
NCLSBd-2	1.4	0.9
NCLSBd-4	1.2	0.9

along with a well-pronounced equilibrium plateau modulus [39]. Such a strong indication for network formation can not be observed here. This might be due to the broad molar mass distribution of PA-12. The difference in the slopes of G' in the terminal region of the master curves of the nanocomposites containing 2 and 4 wt% chemically bonded minerals (prepared by identical swelling methods) is the result of the different molar masses. In the case of the systems with LSB, the slope is between 1.2 (NCLSBd-4) and 1.4 (NCLSBd-2). The values of the slope are thus caused by the absence of chain-length regulators, which leads to similar molar masses independent of the amount of clay added to the nanocomposites (Table 1). The value for NCLSBd-2 is only slightly larger compared to the value for NCLSBd-4.

Since the molar masses and the molar mass distributions of both polyamides containing nonchemically bonded minerals are similar, the smaller slope of NCLSBd-4 can be explained by flow restrictions due to the presence of filler. This obviously happens in such nanocomposites at lower concentrations compared to ordinary particle-filled polymer systems [40]. It might be related to the extremely large surface area of the clay minerals when exfoliated in the polymer matrix.

Conclusions

It is demonstrated that the rheological behavior of PA-12 nanocomposites is very complex. Master curves can be obtained for all pure polyamides and for all nanocomposites. The slopes of the master curves of G' and G'' in the terminal region are considerably lower than those of matrix polyamides with similar molar masses and molar mass distributions. Thus, a superstructure is formed in the nanocomposites in the molten state. This also results in an increase in the viscosity and might have serious implications on the processability of nanocomposites. In the case where the silicate layers are not chemically bonded to the polymer matrix, it is observed that the rheology is mainly governed by the molar masses of the matrix and only to a minor extent by the silicate loading in the range between 2 and 4 wt%. Nevertheless, these small amounts are not negligible for the flow behavior probably caused by the extremely large internal surface.

Acknowledgements We thank T.J. Menke for the WAXS measurements. Süd-Chemie, Germany, supplied the LSB sample. B. Hoffmann thanks R. Mülhaupt for the possibility to work in his group. J. Kressler was supported by the Deutsche Forschungsgemeinschaft and the Fonds der Chemischen Industrie.

References

1. Katz HS, Milewski JV (1987) Handbook of fillers for plastics. Van Nostrand Reinhold, New York
2. Laura RD, Cloos P (1975) Clays Clay Miner 23:343
3. Martin-Rubi JA, Rausell-Colom JA, Serratosa JM (1974) Clays Clay Miner 22:87
4. Usuki A, Kawasumi M, Kojima Y, Okada A, Kurauchi T, Kamigaito O (1993) J Mater Res 8:1174
5. Giannelis EP, Mehrotra V, Tse O, Vaia RA, Sung TC (1992) Mater Res Soc Symp Proc 267:969
6. Giannelis EP (1992) J Miner 44:28
7. Giannelis EP (1996) Adv Mater 8:29
8. Okada A, Usuki A, Kurauchi T, Kamigaito O (1995) In: Mark JE, Lee CY, Bianci PA (eds) Hybrid organic-inorganic composites. ACS Symposium Series 585. American Chemical Society, Washington, DC, pp 55–65
9. Usuki A, Koiwai A, Kojima V, Kawasumi M, Okada A, Fukushima Y, Kurauchi T, Kamigaito O (1993) J Mater Res 8:1179
10. Kojima Y, Usuki A, Kawasumi M, Fukushima Y, Okada A, Kurauchi T, Kamigaito O (1993) J Mater Res 8:1185
11. Kojima Y, Usuki A, Kawasumi M, Okada A, Kurauchi T, Kamigaito O (1993) J Appl Polym Sci 49:1259
12. Pinnavaia TJ, Lan T, Kaviratna PD, Wang Z, Shi H (1995) Polym Mater Sci 73:117
13. Pinnavaia TJ, Lan T, Wang Z, Shi H (1995) Polym Mater Sci 73:296
14. Kelly P, Akelah A, Qutubuddin S, Moet A (1994) J Mater Sci 29:2274
15. Vaia RA, Isii H, Giannelis EP (1993) Chem Mater 5:1694
16. Moet AS, Akelah A (1993) Mater Lett 18:97
17. Moet A, Akelah A, Hiltner A, Baer E (1994) Mater Res Soc Symp Proc 351:91
18. Yano K, Usuki A, Okada A, Kurauchi T, Kamigaito O (1993) J Polym Sci Part A Polym Chem 31:2493
19. Biasci L, Aglietto M, Ruggeri G, Ciardelli F (1994) Polymer 35:3296
20. Lee DC, Jang LW (1996) J Appl Polym Sci 61:1117
21. Messersmith PB, Giannelis EP (1995) J Polym Sci Part A Polym Chem 33:1047
22. Usuki A, Kato M, Okada A, Kurauchi T (1996) J Appl Polym Sci 63:137
23. Kawasumi M, Hasegawa N, Kato M, Usuki A, Okada A (1997) Macromolecules 30:6333
24. Reichert P, Kressler J, Thomann R, Mülhaupt R, Stöppelmann G (1998) Acta Polym 49:116
25. Giannelis EP, Krishnamoorti R, Manias E (1999) Adv Polym Sci 138:107
26. Krishnamoorti R, Giannelis EP (1997) Macromolecules 30:4097
27. Ferry JD (1980) Viscoelastic properties of polymers, 3rd edn. Wiley, New York
28. Macosko CW (1994) Rheology: principles, measurements and application. VCH, New York
29. CO-OP Chemical Co, Tokyo, Japan, Synthetic Mica, Micromica
30. Jasmund K, Lagaly G (eds) (1993) Tonminerale und Tone. Steinkopff, Darmstadt
31. Vogt K (1980) Geol Jahrb Reihe D 39:47
32. Vogt K, Köster HM (1978) Clay Miner 13:25
33. Pezzin G, Gechele GB (1964) J Appl Polym Sci 8:219
34. Laun HM (1979) Rheol Acta 18:478
35. Khanna YP, Han PK, Day ED (1996) Polym Eng Sci 36:1745

36. Kato C, Kuroda K, Misawa M (1979) Clays Clay Miner 27:129
37. Hackett E, Manias E, Giannelis EP (1998) J Chem Phys 108:7410
38. Eckstein A, Friedrich Chr, Lobbrecht A, Spitz R, Mülhaupt R (1997) Acta Polym 48:41
39. Hoffmann B, Dietrich C, Thomann R, Friedrich Chr, Zilg C, Mülhaupt R (eds) (2000) Macromol Rapid Commun 21:57
40. Friedrich Chr, Scheuchenpflug W, Neuhäusler S, Rösch J (1995) J Appl Polym Sci 57:499